

## A variational formulation of the polarizable continuum model

Filippo Lipparini, Giovanni Scalmani, Benedetta Mennucci, Eric Cancès, Marco Caricato, and Michael J. Frisch

Citation: *The Journal of Chemical Physics* **133**, 014106 (2010); doi: 10.1063/1.3454683

View online: <http://dx.doi.org/10.1063/1.3454683>

View Table of Contents: <http://scitation.aip.org/content/aip/journal/jcp/133/1?ver=pdfcov>

Published by the [AIP Publishing](#)

---

### Articles you may be interested in

[A molecularly based theory for electron transfer reorganization energy](#)

*J. Chem. Phys.* **143**, 224502 (2015); 10.1063/1.4936586

[Solvent effects in time-dependent self-consistent field methods. II. Variational formulations and analytical gradients](#)

*J. Chem. Phys.* **143**, 054305 (2015); 10.1063/1.4927167

[Development of a methodology to compute solvation free energies on the basis of the theory of energy representation for solutions represented with a polarizable force field](#)

*J. Chem. Phys.* **137**, 214503 (2012); 10.1063/1.4769075

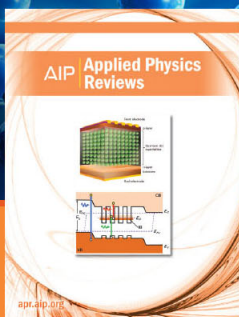
[Multiconfigurational self-consistent field linear response for the polarizable continuum model: Theory and application to ground and excited-state polarizabilities of para-nitroaniline in solution](#)

*J. Chem. Phys.* **119**, 5818 (2003); 10.1063/1.1603728

[Solvation and reorganization energies in polarizable molecular and continuum solvents](#)

*J. Chem. Phys.* **106**, 2372 (1997); 10.1063/1.473790

---



**NEW Special Topic Sections**

**NOW ONLINE**  
Lithium Niobate Properties and Applications:  
Reviews of Emerging Trends

**AIP** | Applied Physics  
Reviews

## A variational formulation of the polarizable continuum model

Filippo Lipparini,<sup>1,2,a)</sup> Giovanni Scalmani,<sup>3</sup> Benedetta Mennucci,<sup>2</sup> Eric Cancès,<sup>4</sup> Marco Caricato,<sup>3</sup> and Michael J. Frisch<sup>3</sup>

<sup>1</sup>*Scuola Normale Superiore, Piazza dei Cavalieri 7, 56126 Pisa, Italy*

<sup>2</sup>*Dipartimento di Chimica e Chimica Industriale, Università di Pisa, Via Risorgimento 35, 56126 Pisa, Italy*

<sup>3</sup>*Gaussian, Inc., 340 Quinipiac Street, Building 40, Wallingford, Connecticut 06492, USA*

<sup>4</sup>*CERMICS, Project-Team Micmac, INRIA-Ecole des Ponts, Université Paris-Est, 6 and 8 Avenue Blaise Pascal, 77455 Marne-la-Vallée Cedex 2, France*

(Received 15 March 2010; accepted 24 May 2010; published online 7 July 2010)

Continuum solvation models are widely used to accurately estimate solvent effects on energy, structural and spectroscopic properties of complex molecular systems. The polarizable continuum model (PCM) is one of the most versatile among the continuum models because of the variety of properties that can be computed and the diversity of methods that can be used to describe the solute from molecular mechanics (MM) to sophisticated quantum mechanical (QM) post-self-consistent field methods or even hybrid QM/MM methods. In this contribution, we present a new formulation of PCM in terms of a free energy functional whose variational parameters include the continuum polarization (represented by the apparent surface charges), the solute's atomic coordinates and—possibly—its electronic density. The problem of finding the optimized geometry of the (polarized) solute, with the corresponding self-consistent reaction field, is recast as the minimization of this free energy functional, simultaneously with respect to all its variables. The numerous potential applications of this variational formulation of PCM are discussed, including simultaneous optimization of solute's geometry and polarization charges and extended Lagrangian dynamics. In particular, we describe in details the simultaneous optimization procedure and we include several numerical examples. © 2010 American Institute of Physics. [doi:10.1063/1.3454683]

### I. INTRODUCTION

The great success achieved in recent years by continuum solvation models<sup>1</sup> in the description of properties and processes of solvated molecular systems is a clear indication of the maturity reached by these methods both in their theoretical formulation and computational implementation. Nowadays, continuum solvation models are available in most computational packages for molecular modeling, both at classical and quantum mechanical (QM) levels of description. In addition, they have been extended in many different directions so that they are no more limited to calculations of solvation energies, but they can be applied to study chemical and biochemical reactivity, molecular spectroscopy, and many other processes in solution. At the same time, continuum solvation models have been extended to simulate not only standard isotropic liquids, but also much more complex environments such as liquid crystals, polymeric matrices, interphases, and even metal particles.<sup>2</sup>

One of the distinct advantages of continuum solvation models is that they do not need any configurational averaging over explicit solvent molecules because such an average is implicitly taken into account in the macroscopic properties used to characterize the solvent. This is also one of the main reasons why continuum solvation models are particularly attractive from the computational standpoint. Another important feature is the fact that they provide a very accurate and computationally affordable way to treat the long-range elec-

trostatic forces. At the same time they can easily include those polarization effects which are often neglected in explicit approaches to solvation modeling, for instance in molecular dynamics (MD) simulations, because of the added computational cost their description would entail. For all these reasons, continuum solvation models are particularly appealing and effective, as compared to other approaches based on an explicit description of the individual solvent molecules, whenever the interest is focused not on the properties of the system as a whole, but rather on the effects that the immediate environment at the microscopic level has on a specific subset of the system, e.g., a single solute molecule, a cluster, or any other supramolecular entity.

Among the most successful and widely used continuum solvent models, the polarizable continuum model (PCM)<sup>1,3,4</sup> exploits an apparent surface charge (ASC) density  $\sigma(\mathbf{s})$  to represent the polarization of the dielectric continuum. The ASC density  $\sigma(\mathbf{s})$  is placed on the surface of a cavity defined by the solute-solvent interface and containing the solute (a single molecule or—as previously noted—a more complex entity). Once a solute-solvent interface has been defined, an integral equation to determine  $\sigma(\mathbf{s})$  can be formulated using the electrostatic properties of the solute's charge density  $\rho(\mathbf{r})$  at the surface. The standard approach for the numerical solution of such equation is to discretize the solute-solvent interface in a collection of surface elements. This turns the integral equation for  $\sigma(\mathbf{s})$  into a set of coupled linear equations whose unknowns  $\{q_i\}$  are the expansion coefficients that provide the optimal representation of  $\sigma(\mathbf{s})$  within a cer-

<sup>a)</sup>Electronic mail: f.lipparini@sns.it.

tain basis set. These coefficients can be regarded as polarization charges located at the representative points of the surface elements, whose interaction with  $\rho(\mathbf{r})$  amounts to twice the electrostatic component of the free energy of solvation, as an equivalent measure of energy is spent to polarize the dielectric. If the method used to describe the charge density  $\rho(\mathbf{r})$  allows for the solute to be polarized, then PCM is able to account for the mutual polarization of solute and dielectric continuum, i.e., implicitly provides a route for the variational minimization of the parameters involved in the description of both  $\rho(\mathbf{r})$  and  $\sigma(\mathbf{s})$ . Recently, a continuous surface charge (CSC) formalism<sup>5</sup> has been established for the formulation and the practical implementation of the PCM models, which is robust, smooth, and free of the singularities and the discontinuities typically introduced by the discretization of the solute-solvent interface.

In this paper we present a new variational formulation of the PCM model in which the PCM charges  $\{q_i\}$  are *not* determined by solving the proper coupled linear equations for each solute's geometry and/or at each iteration of the *self-consistent field* (SCF) procedure (involved in most QM descriptions of the solute electronic density). On the contrary, in the present variational formulation, the solute's atomic coordinates, its electronic density, and the PCM polarization charges  $\{q_i\}$  are treated on the *same* footing and simultaneously as *independent* variables. This is made possible by defining a proper free energy functional of the solute and continuum dielectric system, which depends on all these variables, and whose full variational minimization leads to the free energy of the (polarized) solute at its equilibrium geometry in solution.

In the literature it is possible to find a few attempts<sup>6–14</sup> to reformulate the solution of Poisson's equation as the variational minimization of a functional (see Ref. 6 for a detailed discussion). Among the functionals proposed in the literature, to the best of our knowledge, the one proposed by Attard<sup>13,14</sup> is the only free energy functional suitable for an ASC approach to continuum solvation, being the independent polarization variable a surface charge distribution rather than a three-dimensional vector field, charge distribution, or potential.

With respect to previously proposed ones, the PCM free energy functional we introduce in this paper has several distinct advantages. First of all, it provides a valid definition of the energy for the system also away from the minimum in each of the sets of variables, i.e., also for a polarization of the continuum dielectric which is not in equilibrium with the solute's charge distribution (in the sense that it does not satisfy Poisson's and associated PCM integral equations). Second, it fully maintains the generality of the PCM family of models in the sense that it can be formulated, as described in Ref. 5, independently of the details of the definition and discretization of the solute-solvent interface, and it can as well be applied to the calculation of molecular structural and spectroscopical properties. Moreover, in the limit of high dielectric constants, the corresponding free energy functional and associated integral equation for the "conductorlike" model<sup>15,16</sup> are naturally recovered. From the point of view of efficiency, the evaluation of the PCM free energy functional

and its derivatives with respect to the different groups of variables can be formulated so that no computationally expensive operation, like matrix inversion, is required. Finally, the PCM free energy functional is proved to be free of discontinuities with respect to changes in the total surface area of the solute-solvent interface due to changes in the position of the atoms of the solute, i.e., with changes in the number of surface elements in contact with the dielectric continuum. The functional maintains its continuity even as the changes in the solute-solvent interface take place when the polarization variables are not optimized and thus do not satisfy the PCM equations.

The potential applications of the PCM free energy functional are extremely promising. First, it will allow for the simultaneous optimization with respect to the geometry of the solute, its electronic density, and the polarization charges. Such a strategy is likely to be appealing whenever a cheap method is used to describe the solute [a semiempirical method or molecular mechanics (MM)], where the cost of solving the PCM equations is presently by far the most expensive step in the calculation. This is also relevant in QM/MM calculations, e.g., according to the ONIOM scheme,<sup>17–19</sup> since the most effective geometry optimization strategies involve the full relaxation of the geometry of the MM layer after each step in the QM region.<sup>20</sup> The MM layer is typically the largest part of the real system and the one with the largest contact surface with the dielectric continuum, so that a simultaneous approach to the optimization of geometry and polarization would be most beneficial. Another area of application of a PCM free energy functional is state-specific excited state solvation and, more generally, the evaluation of the self-consistent reaction field corresponding to a post-SCF one-particle density matrix, where the presence of the dielectric continuum couples the various terms (SCF density, molecular orbital relaxation terms, amplitudes of excited determinants, etc.) contributing to the one-particle density.<sup>21–24</sup> A Lagrangian formulation of these post-SCF methods including the PCM free energy functional would constitute a promising route toward the simultaneous variational minimization of all the parameters involved in the calculation of the free energy in solution. Finally, an extended Lagrangian MD method can be derived from the PCM free energy functional,<sup>6,25</sup> in which the polarization charges become dynamical variables with their own fictitious mass. Such an approach could be further extended by coupling it with methods like Car–Parrinello<sup>26</sup> or atom-centered density matrix propagation<sup>27</sup> where also the electronic degrees of freedom are propagated as dynamical variables with a suitable fictitious mass.

Among the potential applications listed above, in this paper we limit our discussion to the specific case of the simultaneous optimization of geometry and polarization, when the solute is described at the MM level. In this way we are able to focus our attention on the details of the continuum solvent model, without additional complications arising from the description of the solute's charge density at the QM level or the introduction of the explicit time evolution of the variables involved in the evaluation of the free energy functional.

Further extensions of the formalism and the implementation to more advanced applications are being actively investigated.

The paper is organized as follows. In Sec. II we first describe the variational formulation of the PCM model in terms of integral operators. Then we introduce the discretization of the solute-solvent interface and we translate the PCM free energy functional into a more practical matrix expression. We show that there are no discontinuities arising from changes in the geometry of the solute from the PCM energy functional. Lastly, we describe the derivatives of the free energy functional with respect to all the variables it depends on and the corresponding working expressions for their efficient evaluation. In Sec. III we report the results of some example calculations, including in particular simultaneous optimizations of the geometry of the solute and of the PCM discretized surface charge density.

## II. A VARIATIONAL FORMULATION OF THE PCM MODEL

In this section we introduce a common formal framework for a variational formulation of the PCM models. We start from the definition of the physical problem in terms of integral operators, then we introduce an optimal discretization of the solute-solvent interface, according to the CSC formalism,<sup>5</sup> which is both robust and smooth with respect to changes in the parameters defining the model. A new version of the PCM equations is obtained, which is equivalent for all practical purposes to the existing ones, but has the distinct advantage of being best suited to reformulate the PCM problem as an actual variational minimization of a free energy functional which includes both the solute's internal energy and its interaction with the solvent. In the following we will focus our attention only on the terms explicitly associated with the solvent and assume that the solute's internal energy is computed according to the proper functional corresponding to the level of theory being used. The free energy functional introduced here is then proved to be free of discontinuities with respect to changes in the solute's geometry, so that it can be applied to describe situations where the solvent polarization and the solute's geometry change independently. Finally, the derivatives of the PCM free energy functional with respect to both the atomic positions of the solute and the solvent polarization variables are described.

### A. PCM energy functional in terms of integral operators

The PCM model solves the Poisson equation in the presence of a dielectric medium outside a cavity  $C$  which hosts the solute. The surface  $\Gamma = \partial C$  is the boundary of this cavity and represents the interface between solute and solvent. The electrostatic potential  $\varphi(\mathbf{r})$  is the solution of Poisson's equation<sup>28</sup>

$$\nabla \cdot [\varepsilon(\mathbf{r}) \nabla \varphi(\mathbf{r})] = -4\pi\rho(\mathbf{r}), \quad (1)$$

where  $\rho(\mathbf{r})$  is the nuclear and electronic charge density of the solute, and the dielectric constant function assumes, for a homogeneous solvent, the simple form

$$\varepsilon(\mathbf{r}) = \begin{cases} 1 & \mathbf{r} \in C \\ \varepsilon & \mathbf{r} \notin C, \end{cases} \quad (2)$$

where  $\varepsilon$  is the macroscopic dielectric permittivity of the solvent. Using Eq. (2) and the appropriate boundary conditions, the problem in Eq. (1) is solved, and the polarization of the medium is represented by an ASC density  $\sigma(\mathbf{s})$  with  $\mathbf{s} \in \Gamma$  (see Ref. 1, Sec. 1.2 for details). The ASC density is the solution of an integral equation whose form varies according to which member of the PCM family of models is being used. The integral equation formalism-PCM (IEF-PCM)<sup>29,30</sup> (hereafter simply called "PCM") is the model of choice because of its broader applicability to all values of  $\varepsilon$ , and because it represents the optimal compromise between accuracy and formal complexity. The integral equation for the PCM model reads

$$\left( \frac{\varepsilon+1}{\varepsilon-1} \hat{\mathcal{I}} - \frac{1}{2\pi} \hat{\mathcal{D}} \right) \hat{\mathcal{S}}\sigma(\mathbf{s}) = - \left( \hat{\mathcal{I}} - \frac{1}{2\pi} \hat{\mathcal{D}} \right) \Phi(\mathbf{s}), \quad (3)$$

where  $\Phi(\mathbf{r})$  is the solute's electrostatic potential,  $\hat{\mathcal{I}}$  is the identity operator, while  $\hat{\mathcal{S}}$  and  $\hat{\mathcal{D}}$  (together with its adjoint  $\hat{\mathcal{D}}^*$ ) are components of the so-called Calderon projector.<sup>31</sup> Their expressions are defined as

$$\hat{\mathcal{S}}\sigma(\mathbf{s}) = \int_{\Gamma} \frac{\sigma(\mathbf{s}')}{|\mathbf{s} - \mathbf{s}'|} d^2\mathbf{s}', \quad (4)$$

$$\hat{\mathcal{D}}^*\sigma(\mathbf{s}) = \int_{\Gamma} \left\{ \frac{\partial}{\partial \hat{\mathbf{n}}_{\mathbf{s}}} \frac{1}{|\mathbf{s} - \mathbf{s}'|} \right\} \sigma(\mathbf{s}') d^2\mathbf{s}', \quad (5)$$

$$\hat{\mathcal{D}}\sigma(\mathbf{s}) = \int_{\Gamma} \left\{ \frac{\partial}{\partial \hat{\mathbf{n}}_{\mathbf{s}'}} \frac{1}{|\mathbf{s} - \mathbf{s}'|} \right\} \sigma(\mathbf{s}') d^2\mathbf{s}', \quad (6)$$

where  $\hat{\mathbf{n}}_{\mathbf{s}}$  is the outward normal direction to the surface at point  $\mathbf{s} \in \Gamma$ .

The formalism described in the following paragraphs is fairly general and it applies to any integral equation of the form

$$\hat{\mathcal{T}}\sigma(\mathbf{s}) = -\hat{\mathcal{R}}\Phi(\mathbf{s}) \quad (7)$$

under the conditions that (i)  $\hat{\mathcal{T}} = p_1(\hat{\mathcal{D}})\hat{\mathcal{S}}$  and  $\hat{\mathcal{R}} = p_2(\hat{\mathcal{D}})$ , where  $p_1$  and  $p_2$  are two polynomials; (ii)  $\hat{\mathcal{R}}$  and  $\hat{\mathcal{T}}$  are both invertible; and (iii)  $\hat{\mathcal{R}}^{-1}\hat{\mathcal{T}}$  is a positive definite operator on the Hilbert space  $L^2(\Gamma)$ . It can be proved that these assumptions are satisfied for IEF-PCM, as well as for Surface and Simulation of Volume Polarization for Electrostatics (SS(V)PE) (Ref. 32) and the Conductor-like PCM (C-PCM).<sup>33</sup> In the case of C-PCM model,  $\hat{\mathcal{T}} = \hat{\mathcal{S}}$  and  $\hat{\mathcal{R}} = c\hat{\mathcal{I}}$ , where  $c$  is a multiplicative constant. The Calderon's projector component  $\hat{\mathcal{S}}$  is a positive definite self-adjoint operator; moreover, the operators  $\hat{\mathcal{S}}$ ,  $\hat{\mathcal{D}}$ , and  $\hat{\mathcal{D}}^*$  satisfy the commutation rule

$$\hat{\mathcal{D}}\hat{\mathcal{S}} = \hat{\mathcal{S}}\hat{\mathcal{D}}^*. \quad (8)$$

Note that, in addition to being positive definite, the operator  $\hat{\mathcal{R}}^{-1}\hat{\mathcal{T}}$  is also self-adjoint since

$$\begin{aligned}
[\hat{\mathcal{R}}^{-1}\hat{\mathcal{T}}]^\dagger &= [p_2(\hat{\mathcal{D}})^{-1}p_1(\hat{\mathcal{D}})\hat{\mathcal{S}}]^\dagger \\
&= \hat{\mathcal{S}}p_1(\hat{\mathcal{D}}^*)p_2(\hat{\mathcal{D}}^*)^{-1} \\
&= p_2(\hat{\mathcal{D}})^{-1}p_1(\hat{\mathcal{D}})\hat{\mathcal{S}} \\
&= \hat{\mathcal{R}}^{-1}\hat{\mathcal{T}}.
\end{aligned} \tag{9}$$

As a consequence of these properties of the  $\hat{\mathcal{R}}^{-1}\hat{\mathcal{T}}$  operator, the PCM free energy functional, i.e., the PCM contribution to the free energy in solution,

$$\mathcal{G}(\sigma) = \frac{1}{2}\langle\sigma, (\hat{\mathcal{R}}^{-1}\hat{\mathcal{T}})\sigma\rangle_\Gamma + \langle\Phi, \sigma\rangle_\Gamma, \tag{10}$$

is strictly convex and it has a unique minimum for  $\sigma = \sigma_0$ . In Eq. (10) we introduced the following notation to indicate the inner product in the Hilbert space  $L^2(\Gamma)$ :

$$\langle f, g \rangle_\Gamma = \int_\Gamma f(\mathbf{s})g(\mathbf{s})d^2s. \tag{11}$$

The minimum of the functional in Eq. (10) can be easily found by setting to zero the functional derivative

$$\left. \frac{\delta\mathcal{G}}{\delta\sigma} \right|_{\sigma=\sigma_0} = (\hat{\mathcal{R}}^{-1}\hat{\mathcal{T}})\sigma_0 + \Phi = 0 \rightarrow (\hat{\mathcal{R}}^{-1}\hat{\mathcal{T}})\sigma_0 = -\Phi, \tag{12}$$

which corresponds to the solution of an integral equation that has only the solute's potential  $\Phi(\mathbf{r})$  as right hand side and it is equivalent to Eq. (7) since we assumed that  $\hat{\mathcal{R}}$  is invertible. At the minimum, the functional in Eq. (10) gives the well known expression for the PCM contribution to the free energy in solution, i.e.,

$$\mathcal{G}(\sigma_0) = \frac{1}{2}\langle\Phi, \sigma_0\rangle_\Gamma. \tag{13}$$

The functional in Eq. (10) is appealing also because of its straightforward physical interpretation. The term linear in  $\sigma(\mathbf{s})$  represents the interaction between the solute and an *arbitrary* polarization in the dielectric medium, while the quadratic term accounts for the unfavorable interaction of the ASC density with itself according to the positive definite, self-adjoint operator  $\hat{\mathcal{R}}^{-1}\hat{\mathcal{T}}$ . In the optimization with respect to  $\sigma(\mathbf{s})$ , the linear term will lower the energy, but it will eventually be balanced by the increase in energy due to the quadratic term.

The practical issue with Eqs. (10) and (12) is the presence of the inverse of the operator  $\hat{\mathcal{R}}$  or the need to invert  $\hat{\mathcal{R}}^{-1}\hat{\mathcal{T}}$  in order to find the optimal ASC density  $\sigma_0$ . However, it is possible to eliminate  $\hat{\mathcal{R}}^{-1}$  altogether through a change of variable as in

$$\sigma = \hat{\mathcal{R}}^\dagger \tilde{\sigma}, \tag{14}$$

which leads to the new functional

$$\begin{aligned}
\tilde{\mathcal{G}}(\tilde{\sigma}) &= \frac{1}{2}\langle\hat{\mathcal{R}}^\dagger\tilde{\sigma}, (\hat{\mathcal{R}}^{-1}\hat{\mathcal{T}})\hat{\mathcal{R}}^\dagger\tilde{\sigma}\rangle_\Gamma + \langle\Phi, \hat{\mathcal{R}}^\dagger\tilde{\sigma}\rangle_\Gamma \\
&= \frac{1}{2}\langle\tilde{\sigma}, (\hat{\mathcal{T}}\hat{\mathcal{R}}^\dagger)\tilde{\sigma}\rangle_\Gamma + \langle\hat{\mathcal{R}}\Phi, \tilde{\sigma}\rangle_\Gamma,
\end{aligned} \tag{15}$$

where  $\hat{\mathcal{T}}\hat{\mathcal{R}}^\dagger$  is also a self-adjoint and positive definite opera-

tor and the above defined functional admits the stationary condition

$$\left. \frac{\delta\tilde{\mathcal{G}}}{\delta\tilde{\sigma}} \right|_{\tilde{\sigma}=\tilde{\sigma}_0} = (\hat{\mathcal{T}}\hat{\mathcal{R}}^\dagger)\tilde{\sigma}_0 + \hat{\mathcal{R}}\Phi = 0, \tag{16}$$

which leads to an optimal  $\tilde{\sigma}_0 = (\hat{\mathcal{R}}^\dagger)^{-1}\sigma_0$ . Since, as long as Eq. (14) holds,

$$\mathcal{G}(\sigma) = \tilde{\mathcal{G}}(\tilde{\sigma}), \tag{17}$$

it is possible to evaluate the PCM contribution to the free energy using Eq. (15) which depends on  $\tilde{\sigma}$  and does not require the  $\hat{\mathcal{R}}^{-1}$  operator.

## B. PCM energy functional in terms of discretized solute-solvent interface

Practical applications of all PCM models require a discrete representation of the ASC density over the solute-solvent interface  $\Gamma$ . According to the CSC formalism presented in details elsewhere,<sup>5,34</sup> the solute-solvent interface is discretized in  $n_g$  surface elements characterized by their position  $\mathbf{s}_i$ , their surface area  $a_i$ , and their outward normal direction  $\hat{\mathbf{n}}_i$ . In addition to these basic geometrical quantities, each surface element is also characterized by a *self-potential* factor  $f_i$  and a *self-field* factor  $g_i$  which are chosen to achieve an optimal discretized representation of the operators in Eqs. (4)–(6). The position and the area of the surface elements are fixed according to the York–Karplus<sup>7</sup> (YK) discretization scheme. The ASC density  $\sigma(\mathbf{s})$  is expanded in terms of surface elements basis functions  $\phi_i$ , which are typically simple spherical Gaussian functions,

$$\sigma(\mathbf{r}) = \sum_i \frac{q_i}{a_i} \phi_i(\mathbf{r}; \mathbf{s}_i, \zeta_i), \tag{18}$$

so that each surface is also characterized at least by an optimally chosen exponent  $\zeta_i$  for the basis function. The quantities  $\{q_i\}$  are the expansion coefficients of the ASC, i.e., the variational parameters, and correspond to the polarization charges. The discrete representation of the  $\hat{\mathcal{S}}$ ,  $\hat{\mathcal{D}}$ , and  $\hat{\mathcal{D}}^*$  operators<sup>5,35</sup> is achieved through the definition of the  $\mathbf{S}$  matrix

$$\begin{cases} S_{ii} = \frac{f_i}{a_i} \\ S_{ij} = \langle i|j \rangle \end{cases} \tag{19}$$

and the  $\mathbf{D}^*$  and  $\mathbf{D}$  matrices

$$\begin{cases} D_{ii}^* = \frac{g_i}{a_i} \\ D_{ij}^* = -\hat{\mathbf{n}}_i \cdot \frac{\partial}{\partial \mathbf{s}_i} \langle i|j \rangle, \end{cases} \tag{20}$$

$$\begin{cases} D_{ii} = \frac{g_i}{a_i} \\ D_{ij} = -\frac{\partial}{\partial \mathbf{s}_j} \langle i|j \rangle \cdot \hat{\mathbf{n}}_j, \end{cases} \tag{21}$$

where the *braket* notation is used to indicate the integral

$$\langle i|j\rangle = \iint \frac{\phi_i(\mathbf{r}; \mathbf{s}_i, \zeta_i) \phi_j(\mathbf{r}'; \mathbf{s}_j, \zeta_j)}{|\mathbf{r} - \mathbf{r}'|} d^3\mathbf{r} d^3\mathbf{r}', \quad (22)$$

which is a standard two-center electron repulsion integral.

Using the definitions in Eqs. (19)–(21), the matrices representing the operators  $\hat{\mathcal{R}}$  and  $\hat{\mathcal{T}}$  can be written as<sup>34</sup>

$$\mathbf{R}_\varepsilon = \frac{\varepsilon + 1}{\varepsilon - 1} \mathbf{1} - \frac{1}{2\pi} \mathbf{D}\mathbf{A} \quad (23)$$

and

$$\mathbf{T}_\varepsilon = \mathbf{R}_\varepsilon \mathbf{S}, \quad (24)$$

where  $(\mathbf{A})_{ij} = a_i \delta_{ij}$  is the diagonal matrix collecting the values of the area of the surface elements. Also, by formally taking the limit for  $\varepsilon \rightarrow \infty$  one obtains

$$\mathbf{R}_\infty = \lim_{\varepsilon \rightarrow \infty} \mathbf{R}_\varepsilon = \mathbf{1} - \frac{1}{2\pi} \mathbf{D}\mathbf{A}. \quad (25)$$

Using the above definitions, the PCM integral equations in Eqs. (3) and (7) can be written as

$$\mathbf{T}_\varepsilon \mathbf{q} = -\mathbf{R}_\infty \mathbf{V}, \quad (26)$$

where the vector  $V_i = \Phi(s_i)$  collects the values of the solute's electrostatic potential at the surface elements.

Using currently available discretization schemes, the representation of the operators in Eqs. (4)–(6), i.e., the matrices defined in Eqs. (19)–(21), does not enjoy the same formal properties of the corresponding operators. In particular, they do not satisfy exactly the commutation rule set forth in Eq. (8) which in discretized form reads

$$\mathbf{D}\mathbf{A}\mathbf{S} \approx \mathbf{S}\mathbf{A}\mathbf{D}^*. \quad (27)$$

This led to the realization that Eq. (7) can be represented using an arbitrary combination of  $\mathbf{T}_\varepsilon$  and  $\mathbf{T}_\varepsilon^\dagger$ . In particular, three of such combinations are noteworthy and have been described in the literature, namely,

$$\mathbf{R}_\varepsilon \mathbf{S} \mathbf{q} = -\mathbf{R}_\infty \mathbf{V}, \quad (28)$$

$$\mathbf{S} \mathbf{R}_\varepsilon^\dagger \mathbf{q} = -\mathbf{R}_\infty \mathbf{V}, \quad (29)$$

$$\frac{1}{2} (\mathbf{R}_\varepsilon \mathbf{S} + \mathbf{S} \mathbf{R}_\varepsilon^\dagger) \mathbf{q} = -\mathbf{R}_\infty \mathbf{V}. \quad (30)$$

They produce three different sets of polarization charges and correspond to three different free energies. Typically, these energy differences are well below 1 kcal mol<sup>-1</sup> and they appear to be smaller for less polar solvents where, however, the overall solute-solvent interaction energy is also smaller. Unfortunately, these differences are difficult to reduce or remove in a controllable or predictable way, simply by increasing the number of the surface elements. Rather, they depend on other details of the discretization scheme being used, such as the choice of the diagonal elements of the  $\mathbf{S}$ ,  $\mathbf{D}^*$ , and  $\mathbf{D}$  matrices, i.e., the representation of the integrable singularities in Eqs. (4)–(6). The first derivation<sup>36</sup> of the IEF-PCM equations was done as in Eq. (29). On the other hand, some authors argued that Eq. (30) is more convenient because the PCM linear system is a symmetric one.<sup>32,37</sup> Other authors<sup>34,38</sup>

choose Eq. (28) because it naturally goes to the right limit for  $\varepsilon \rightarrow \infty$ , i.e.,

$$\lim_{\varepsilon \rightarrow \infty} (\mathbf{R}_\varepsilon \mathbf{S} \mathbf{q}) = \mathbf{R}_\infty \mathbf{S} \mathbf{q} = -\mathbf{R}_\infty \mathbf{V} \rightarrow \mathbf{S} \mathbf{q} = -\mathbf{V}, \quad (31)$$

which is equivalent to the limit for  $\varepsilon \rightarrow \infty$  of the conductor-like model C-PCM.<sup>39</sup>

Following the formalism introduced in Sec. II A, our goal is to obtain a discretized version of the free energy functional defined in Eq. (10) that preserves the properties we mentioned previously. In particular, the two terms in the functional must have the usual physical interpretation of solute-solvent and solvent-solvent interaction, the corresponding PCM equations must have on the left hand side a symmetric matrix and the right hand side should involve just the solute's potential. Note that making use of Eq. (30), as suggested by some authors,<sup>37</sup> is not enough to preserve these properties of the free energy functional in Eq. (10), although a similar functional can be written and used for a variational solution of the associated PCM equations.

Thus, by means of the same procedure described in Sec. II A, we first rearrange Eq. (26) as follows:

$$(\mathbf{R}_\infty^{-1} \mathbf{T}_\varepsilon) \mathbf{q} = \mathbf{X} \mathbf{q} = -\mathbf{V}, \quad (32)$$

and then we *symmetrize* the matrix on the left hand side, thereby *redefining* the PCM linear system as

$$\left( \frac{\mathbf{R}_\infty^{-1} \mathbf{T}_\varepsilon + \mathbf{T}_\varepsilon^\dagger (\mathbf{R}_\infty^{-1})^\dagger}{2} \right) \mathbf{q} = \left( \frac{\mathbf{X} + \mathbf{X}^\dagger}{2} \right) \mathbf{q} = \tilde{\mathbf{X}} \mathbf{q} = -\mathbf{V}, \quad (33)$$

which is now a symmetric linear system and has only the potential on the right hand side. Note that, for the same reason why there are various possible discrete representations of Eq. (7), one can also introduce two alternative versions of Eq. (33), namely,  $\mathbf{X} \mathbf{q} = -\mathbf{V}$  and  $\mathbf{X}^\dagger \mathbf{q} = -\mathbf{V}$ . These two equations, together with Eq. (33) and Eqs. (28)–(30), represent six different discretized versions of the same PCM problem in operator form as in Eq. (7). All these different versions provide the same result in the limit of an exact quadrature. However, given a finite discretization scheme, we believe it is better to use from now on Eq. (33) as definition of the PCM model, as it is the only form among the six mentioned here that involves both a symmetric matrix and has only the potential on the right hand side.

Although Eq. (33) is the best suited for a variational formulation of the PCM model, the presence of the inverse of the  $\mathbf{R}_\infty$  matrix makes it impractical for production calculations. Thus, as discussed above, we introduce the change of variables

$$\mathbf{q} = \mathbf{R}_\infty^\dagger \tilde{\mathbf{q}}, \quad (34)$$

which leads to the definition of a new set of equations,

$$\left( \frac{\mathbf{T}_\varepsilon \mathbf{R}_\infty^\dagger + \mathbf{R}_\infty \mathbf{T}_\varepsilon^\dagger}{2} \right) \tilde{\mathbf{q}} = \tilde{\mathbf{Y}} \tilde{\mathbf{q}} = -\mathbf{R}_\infty \mathbf{V} = -\tilde{\mathbf{V}}, \quad (35)$$

and a corresponding free energy functional,

$$\mathcal{G}(\tilde{\mathbf{q}}) = \frac{1}{2} \tilde{\mathbf{q}}^\dagger \tilde{\mathbf{Y}} \tilde{\mathbf{q}} + \tilde{\mathbf{q}}^\dagger \tilde{\mathbf{V}} = \frac{1}{2} \tilde{\mathbf{q}}^\dagger \mathbf{Y} \tilde{\mathbf{q}} + \tilde{\mathbf{q}}^\dagger \tilde{\mathbf{V}}. \quad (36)$$

The change of variable in Eq. (34) is a linear transformation of the coordinate system in which the PCM energy functional is expressed. While the  $\{q_i\}$  have a clear physical interpretation, their use for the discretized form of Eq. (10) is impractical as explained above. However, the recombination of the  $\{q_i\}$  into the  $\{\tilde{q}_i\}$  according to the  $\mathbf{R}_\infty^\dagger$  matrix simply provides a more computationally convenient coordinates system, which does not change the physical significance of the free energy functional: in particular, the functional assumes the same value at the minimum and the ASC density distribution can be recovered simply by backtransforming the  $\{\tilde{q}_i\}$  into the  $\{q_i\}$ . Additionally, note that in the quadratic term we can use  $\mathbf{Y} = \mathbf{T}_\varepsilon \mathbf{R}_\infty^\dagger$  instead of  $\tilde{\mathbf{Y}} = \frac{1}{2}(\mathbf{Y} + \mathbf{Y}^\dagger)$  since the pre- and postmultiplication by  $\tilde{\mathbf{q}}$  make irrelevant any contribution from the antisymmetric component of the  $\mathbf{Y}$  matrix.

As discussed in Ref. 5 the choice of the self-potential and self-field factors used in the definition of the  $\mathbf{S}$ ,  $\mathbf{D}^*$ , and  $\mathbf{D}$  matrices in Eqs. (19) and (20) consistently leads to matrices that behave as similarly as possible to the corresponding operators. All the  $f_i$  are positive numbers while all the  $g_i$  are negative and, for the case of a single sphere, the  $\mathbf{S}$  matrix is positive definite and strongly diagonal dominant and the product  $\mathbf{DASAD}^*$  in  $\mathbf{T}_\varepsilon \mathbf{R}_\infty^\dagger$  is also positive definite. In the case of a general cavity made of interlocking spheres, it is difficult to construct an analytical argument, but extensive numerical tests support the same conclusions. Therefore, we expect the  $\tilde{\mathbf{Y}}$  matrix to be positive definite, thus ensuring that  $\mathcal{G}(\tilde{\mathbf{q}})$  has the same properties of the functional defined in Eq. (10) in terms of the integral operators: in particular, that it is strictly convex and therefore admits a unique minimum. Moreover, an *a posteriori* argument in support of this hypothesis is the fact that a very simple minded conjugate gradient optimizer consistently finds a minimum of the functional in Eq. (36) which corresponds to the solution of the linear system in Eqs. (35) and (33) (see Sec. III). Finally, note that the energy functional introduced in Eq. (36) has the correct limit for large values of  $\varepsilon$ , i.e., it goes to the same limit as the C-PCM energy functional<sup>6</sup>

$$\begin{aligned} \lim_{\varepsilon \rightarrow \infty} \mathcal{G}(\tilde{\mathbf{q}}) &= \lim_{\varepsilon \rightarrow \infty} \left( \frac{1}{2} \tilde{\mathbf{q}}^\dagger \mathbf{R}_\infty^{-1} \mathbf{R}_\varepsilon \mathbf{S} \mathbf{R}_\infty^\dagger (\mathbf{R}_\infty^{-1})^\dagger \tilde{\mathbf{q}} + \tilde{\mathbf{q}}^\dagger \mathbf{R}_\infty^{-1} \mathbf{R}_\varepsilon \mathbf{V} \right) \\ &= \frac{1}{2} \tilde{\mathbf{q}}^\dagger \mathbf{S} \tilde{\mathbf{q}} + \tilde{\mathbf{q}}^\dagger \mathbf{V} \\ &= \lim_{\varepsilon \rightarrow \infty} \left( \frac{1}{2f(\varepsilon)} \tilde{\mathbf{q}}^\dagger \mathbf{S} \tilde{\mathbf{q}} + \tilde{\mathbf{q}}^\dagger \mathbf{V} \right), \end{aligned} \quad (37)$$

where  $f(\varepsilon) = (\varepsilon - 1)/\varepsilon$ . The  $\{q_i\}$  provide a good set of coordinates for the minimization of the C-PCM functional and no variable transformation is required.

### C. Continuity with respect to the number of exposed surface elements

Achieving a formally correct and effective expression for the PCM energy functional as in Eq. (36) is only enough for its use in cases when the number of surface elements  $n_g$  exposed to the solvent remains constant. Variational minimi-

zation of Eq. (36), at a fixed solute's geometry, is achieved when the polarization charges satisfy the PCM equations as in Eq. (35), and *only* then Eq. (36) is equivalent to discretized version of Eq. (13), i.e.,

$$\mathcal{G}(\tilde{\mathbf{q}}_0) = \frac{1}{2} \tilde{\mathbf{q}}_0^\dagger \tilde{\mathbf{V}} = \frac{1}{2} \mathbf{V}^\dagger \mathbf{q}_0 = \mathcal{G}(\mathbf{q}_0). \quad (38)$$

In other words, the minimization of  $\mathcal{G}(\tilde{\mathbf{q}})$  with respect to the  $\{\tilde{q}_i\}$  is just an alternative to the solution of the PCM equations, but its usefulness is not immediately evident for applications like simultaneous optimization of geometry and PCM polarization or extended Lagrangian dynamics, i.e., when the atomic positions can change *without* assuming that the PCM equations are satisfied. The key issue in these cases is how to handle the fact that as the geometry changes, the cavity also changes and new surface elements can become exposed to the solvent while existing ones can become buried within the cavity. Clearly what remains constant, even as the geometry changes, is the total number of surface elements  $n_{\text{all}}$  that are generated from the union of the discretized surfaces of all the spheres, irrespective of whether they are exposed or not to the solvent. The difference  $n_{\text{sh}} = n_{\text{all}} - n_g$  is the number of *shadow* elements, i.e., the number of surface elements that, for a given geometry of the solute, lie inside the cavity or—in other words—the surface elements whose weight has been switched down to zero.

The CSC formalism<sup>5</sup> and—in particular—the YK discretization scheme<sup>7</sup> can provide a robust formulation of the free energy functional  $\mathcal{G}(\mathbf{R}, \tilde{\mathbf{q}})$  that depends on both the set of atomic positions  $\{\mathbf{R}_A\}$ , which usually correspond to the location of the centers of the spheres, and the  $\{\tilde{q}_i\}$ . Such functional can be proved to be free of discontinuities as the number of exposed surface elements  $n_g$  changes with  $\{\mathbf{R}_A\}$ . York and Karplus<sup>7</sup> demonstrated the smoothness of the free energy functional in the case of the C-PCM model, by considering an extended system on equations which include also the shadow elements, and a suitably transformed  $\mathbf{S}$  matrix. However, in their work the possibility of treating the polarization charges as true independent variables is only implicit, as they always assume that the functional is stationary with respect to the  $\{q_i\}$

In the following, similar to what was done in Ref. 7, we introduce an extended set of variables<sup>6</sup> which includes all  $n_{\text{all}}$  surface elements (both exposed and shadow elements) so that the total number of polarization variables in  $\mathcal{G}(\mathbf{R}, \tilde{\mathbf{q}})$  cannot change. Hence, we show that there is no discontinuity in the energy functional as the surface elements move in and out of the exposed and the shadow sets, carrying with them  $\tilde{q}_i$  “charges” which may have a value far from optimal. In particular, we address the issue of nonzero polarization charges associated with shadow surface elements, and of their contribution to the free energy. To this end, rather than transforming the  $\tilde{\mathbf{Y}}$  matrix in a way similar to that discussed in Ref. 7, we introduce a further linear transformation of the variables according to

$$\tilde{\mathbf{q}} = \mathbf{A}^{1/2} \bar{\tilde{\mathbf{q}}}. \quad (39)$$

Note that the set of the  $\{\bar{\tilde{q}}_i\}$  has always  $n_{\text{all}}$  elements and  $n_g$  of them correspond to the exposed surface elements. The values

of the  $\{\bar{q}_i\}$  associated with these elements can be related to the values of the  $\{\tilde{q}_i\}$  directly using the inverse of Eq. (39), i.e.,

$$\bar{\mathbf{q}} = \mathbf{A}^{-1/2} \tilde{\mathbf{q}}, \quad (40)$$

which is valid only for the surface elements with  $a_i > 0$ . The remaining  $n_{\text{sh}}$  shadow charges  $\{\bar{q}_{i,\text{sh}}\}$  are not mapped to the exposed surface, they do not “feel” neither the solute potential nor the presence of any other polarization charge, and thus their value is not “controlled” by the laws of electrostatics. Nevertheless, the energy functional  $\mathcal{G}(\mathbf{R}, \bar{\mathbf{q}})$  depends on the shadow charges  $\{\bar{q}_{i,\text{sh}}\}$  and their value should be chosen accordingly to achieve a variational minimization of the energy. To better understand how the functional  $\mathcal{G}(\mathbf{R}, \bar{\mathbf{q}})$  depends on the shadow charges  $\{\bar{q}_{i,\text{sh}}\}$  and to verify that there are no discontinuities, we evaluate the limit as the generic surface element area goes to zero,

$$\lim_{a_i \rightarrow 0} \mathcal{G}(\mathbf{R}, \bar{\mathbf{q}}) = \lim_{a_i \rightarrow 0} \left( \frac{1}{2} \bar{\mathbf{q}}^\dagger \mathbf{A}^{1/2} \mathbf{Y} \mathbf{A}^{1/2} \bar{\mathbf{q}} + \bar{\mathbf{q}}^\dagger \mathbf{A}^{1/2} \tilde{\mathbf{V}} \right). \quad (41)$$

The linear term involving  $\bar{q}_i$  vanishes identically while, considering the definition of the  $\mathbf{Y}$  matrix, the quadratic term in Eq. (41) seems to contain diverging terms due to the form of the diagonal elements of the  $\mathbf{S}$ ,  $\mathbf{D}$ , and  $\mathbf{D}^*$  matrices, while the off-diagonal elements do not diverge as  $a_i$  goes to zero and thus they give no contribution to the limit [see Eqs. (19)–(21)]. A more careful examination of the limit for  $a_i \rightarrow 0$  shows that the diagonal elements contribute the following quantity:

$$\begin{aligned} \lim_{a_i \rightarrow 0} (\bar{\mathbf{q}}^\dagger \mathbf{A}^{1/2} \mathbf{Y} \mathbf{A}^{1/2} \bar{\mathbf{q}}) &= \lim_{a_i \rightarrow 0} \left[ \bar{\mathbf{q}}^\dagger \mathbf{A}^{1/2} \left( \frac{\varepsilon + 1}{\varepsilon - 1} \mathbf{1} - \frac{1}{2\pi} \mathbf{D} \mathbf{A} \right) \mathbf{S} \right. \\ &\quad \left. \times \left( \mathbf{1} - \frac{1}{2\pi} \mathbf{A} \mathbf{D}^* \right) \mathbf{A}^{1/2} \bar{\mathbf{q}} \right] \\ &= \lim_{a_i \rightarrow 0} \left[ \bar{q}_i a_i^{1/2} \left( \frac{\varepsilon + 1}{\varepsilon - 1} - \frac{1}{2\pi} \frac{g_i}{a_i} \right) \frac{f_i}{a_i} \right. \\ &\quad \left. \times \left( 1 - \frac{1}{2\pi} a_i \frac{g_i}{a_i} \right) a_i^{1/2} \bar{q}_i \right] \\ &= \left[ \left( \frac{\varepsilon + 1}{\varepsilon - 1} - \frac{g_i}{2\pi} \right) f_i \left( 1 - \frac{g_i}{2\pi} \right) \right] \bar{q}_{i,\text{sh}}^2 \\ &= \lambda_i \bar{q}_{i,\text{sh}}^2, \end{aligned} \quad (42)$$

where all  $\lambda_i$  are positive numbers since, by definition, all the  $f_i$  are positive while all the  $g_i$  are negative (see Sec. II B). Therefore, there are no divergent terms in the PCM energy functional  $\mathcal{G}(\mathbf{R}, \bar{\mathbf{q}})$  in terms of the  $\{\bar{q}_i\}$  charges, which is thus continuous with respect to changes in the atomic positions  $\{\mathbf{R}_A\}$ . The free energy functional can be written equivalently in two ways,

$$\begin{aligned} \mathcal{G}(\mathbf{R}, \bar{\mathbf{q}}) &= \frac{1}{2} \bar{\mathbf{q}}^\dagger \mathbf{A}^{1/2} \mathbf{Y} \mathbf{A}^{1/2} \bar{\mathbf{q}} + \bar{\mathbf{q}}^\dagger \mathbf{A}^{1/2} \tilde{\mathbf{V}} \\ &= \frac{1}{2} \tilde{\mathbf{q}}^\dagger \mathbf{Y} \tilde{\mathbf{q}} + \tilde{\mathbf{q}}^\dagger \tilde{\mathbf{V}} + \frac{1}{2} \tilde{\mathbf{q}}_{\text{sh}}^\dagger \boldsymbol{\lambda} \tilde{\mathbf{q}}_{\text{sh}}. \end{aligned} \quad (43)$$

Note that the minimum value of the free energy functional  $\mathcal{G}(\mathbf{R}, \bar{\mathbf{q}})$  for a given *solute's geometry* can be reached by

separately minimizing the terms for  $i \in n_g$ , which amounts to solving the PCM equations as in Eq. (35), and the term depending on the shadow charges, which represents a sort of *self-energy* of the uncoupled  $\{\bar{q}_{i,\text{sh}}\}$ . Since all the  $\lambda_i$  coefficients are positive, the minimum energy according to Eq. (44) is achieved when all the  $\{\bar{q}_{i,\text{sh}}\}$  are set to zero, which is consistent with the description of the solvation process according to the PCM model. However, we point out that we want the geometrical and polarization degrees of freedom to be able to evolve *independently*. In particular, during a simultaneous optimization procedure with respect to all variables, a surface element can become buried within the cavity while associated with a nonzero  $\bar{q}_i$  or, on the other hand, a previously buried surface element, whose  $\bar{q}_i$  has been optimized to zero, can become exposed to the solvent and start to interact with the solute and the other surface elements. Therefore, consistent with the use of an extended set of  $n_{\text{all}}$  polarization variables, it is necessary to introduce in the free energy functional a suitable term which depends on the values of the shadow charges. The presence of this term is irrelevant only when the polarization charges satisfy the PCM equations, but not in the case of an arbitrary distribution of  $\{\bar{q}_i\}$ .

Finally, the change of variables to the  $\{\bar{q}_i\}$  set can be exploited also for the C-PCM energy functional, which assumes the form

$$\begin{aligned} \mathcal{G}(\mathbf{R}, \bar{\mathbf{q}}) &= \frac{1}{2f(\varepsilon)} \bar{\mathbf{q}}^\dagger \mathbf{A}^{1/2} \mathbf{S} \mathbf{A}^{1/2} \bar{\mathbf{q}} + \bar{\mathbf{q}}^\dagger \mathbf{A}^{1/2} \mathbf{V} \\ &= \frac{1}{2f(\varepsilon)} \mathbf{q}^\dagger \mathbf{S} \mathbf{q} + \mathbf{q}^\dagger \mathbf{V} + \frac{1}{2} \bar{\mathbf{q}}_{\text{sh}}^\dagger \boldsymbol{\lambda} \bar{\mathbf{q}}_{\text{sh}}. \end{aligned} \quad (44)$$

In this case the change of variable is  $\mathbf{q} = \mathbf{A}^{1/2} \bar{\mathbf{q}}$  and  $\lambda_i = f_i$ , and the equivalence of Eqs. (44) and (43) can easily be proven by taking the limit of both expressions for  $\varepsilon \rightarrow \infty$ . A functional similar to the one in Eq. (44) was already implicit in the work of York and Karplus,<sup>7</sup> although they never wrote explicitly the (possibly nonzero) energy contribution due to the shadow charges and in their derivation  $\boldsymbol{\lambda} = \mathbf{1}$ .

## D. Effective evaluation of the energy functional and its analytical gradient

In sections II A–II C we introduced a formal framework whose major result is a unified variational formulation of the PCM models, which is continuous even as the atoms in the solute move and the surface elements become exposed to the solvent or buried within the solute's cavity. In the following we present the working equations for an effective evaluation of the PCM free energy functional and its derivatives with respect to the atomic positions and the polarization variables  $\{\bar{q}_i\}$ , which allow for the simultaneous optimization of the solute's geometry and the ASC density.

The working expression for the evaluation of the energy functional is Eq. (43); in practice, it is implemented using the equivalent expression

$$\begin{aligned} \mathcal{G}(\mathbf{R}, \bar{\mathbf{q}}) &= \mathcal{G}(\mathbf{R}, \tilde{\mathbf{q}}) + \frac{1}{2} \bar{\mathbf{q}}_{\text{sh}}^{\dagger} \boldsymbol{\lambda} \bar{\mathbf{q}}_{\text{sh}} \\ &= \left[ \mathbf{V} + \mathbf{S} \left( \frac{1}{2} \mathbf{q} + \frac{1}{\varepsilon - 1} \tilde{\mathbf{q}} \right) \right]^{\dagger} \mathbf{q} + \frac{1}{2} \bar{\mathbf{q}}_{\text{sh}}^{\dagger} \boldsymbol{\lambda} \bar{\mathbf{q}}_{\text{sh}}, \end{aligned} \quad (45)$$

where for each exposed surface element  $\tilde{q}_i = a_i^{1/2} \bar{q}_i$ , and where the vector  $\mathbf{q}$  is defined as  $\mathbf{q} = \mathbf{R}_{\infty}^{\dagger} \tilde{\mathbf{q}}$ .

The gradient of the free energy functional in Eq. (45) with respect to the  $\{\bar{q}_{ij}\}$  charges, for a given configuration of the solute's atoms, is

$$\begin{aligned} \frac{\partial \mathcal{G}(\mathbf{R}, \bar{\mathbf{q}})}{\partial \bar{\mathbf{q}}} &= \mathbf{A}^{1/2} \frac{\partial \mathcal{G}(\mathbf{R}, \tilde{\mathbf{q}})}{\partial \tilde{\mathbf{q}}} + \boldsymbol{\lambda} \bar{\mathbf{q}}_{\text{sh}} \\ &= \mathbf{A}^{1/2} \left[ \mathbf{R}_{\infty} \left( \mathbf{V} + \frac{1}{\varepsilon - 1} \mathbf{S} \tilde{\mathbf{q}} + \mathbf{S} \mathbf{q} \right) + \frac{1}{\varepsilon - 1} \mathbf{S} \mathbf{q} \right] + \boldsymbol{\lambda} \bar{\mathbf{q}}_{\text{sh}}, \end{aligned} \quad (46)$$

and it can be assembled with only one contraction of the  $\mathbf{S}$  matrix with two vectors and one contraction of  $\mathbf{D}$  with one vector.<sup>40</sup>

On the other hand, the gradient of the free energy functional in Eq. (45) with respect to the position of the generic atom  $A$  can be written as follows:

$$\begin{aligned} \frac{\partial \mathcal{G}(\mathbf{R}, \bar{\mathbf{q}})}{\partial \mathbf{R}_A} &= \frac{\partial \mathcal{G}(\mathbf{R}, \tilde{\mathbf{q}})}{\partial \mathbf{R}_A} - \frac{1}{2} \tilde{\mathbf{q}}^{\dagger} \left( \mathbf{A}^{-1} \frac{\partial \mathbf{A}}{\partial \mathbf{R}_A} \right) \frac{\partial \mathcal{G}(\mathbf{R}, \tilde{\mathbf{q}})}{\partial \tilde{\mathbf{q}}} \\ &\quad + \frac{1}{2} \bar{\mathbf{q}}_{\text{sh}}^{\dagger} \frac{\partial \boldsymbol{\lambda}}{\partial \mathbf{R}_A} \bar{\mathbf{q}}_{\text{sh}} \\ &= \left( \frac{\partial \mathbf{V}}{\partial \mathbf{R}_A} \right)^{\dagger} \mathbf{q} + \frac{1}{2} \tilde{\mathbf{q}}^{\dagger} \left[ \frac{\partial \mathbf{R}_{\infty}}{\partial \mathbf{R}_A} (2\mathbf{V} + \mathbf{T}_{\varepsilon}^{\dagger} \tilde{\mathbf{q}}) + \frac{\partial \mathbf{T}_{\varepsilon}}{\partial \mathbf{R}_A} \mathbf{q} \right] \\ &\quad - \frac{1}{2} \tilde{\mathbf{q}}^{\dagger} \left( \mathbf{A}^{-1} \frac{\partial \mathbf{A}}{\partial \mathbf{R}_A} \right) \frac{\partial \mathcal{G}(\mathbf{R}, \tilde{\mathbf{q}})}{\partial \tilde{\mathbf{q}}} + \frac{1}{2} \bar{\mathbf{q}}_{\text{sh}}^{\dagger} \frac{\partial \boldsymbol{\lambda}}{\partial \mathbf{R}_A} \bar{\mathbf{q}}_{\text{sh}}, \end{aligned} \quad (47)$$

where the first term on the right hand side represents the direct dependence of the functional on the atomic coordinates while the second term arises from the *indirect* dependence through the derivatives of the linear transformation between  $\bar{\mathbf{q}}$  and  $\tilde{\mathbf{q}}$ , and involves the same intermediate quantity used in Eq. (46). This extra dependence is due to the fact that Eq. (39) involves the area of the surface element, which in turn depends on the position of the atoms, if the surface element lies in the switching region defined according to the YK discretization scheme.<sup>7</sup> Finally, the last term in Eq. (47) is usually zero as long as the radii of the spheres do not depend on the atomic positions, but it should be included in the formal derivation for the sake of generality, and it would be required whether added spheres were to be generated to approximate the solvent excluded surface (SES) by means of the GePol algorithm.<sup>41</sup>

The above expression can be evaluated using the same approach previously developed and implemented for the gradient of the PCM energy corresponding to Eq. (26) and described in Ref. 34. Without repeating here any of the details of the derivation, the final expression obtained in Ref. 34 reads

$$\frac{\partial \mathcal{G}(\mathbf{R}, \mathbf{q})}{\partial \mathbf{R}_A} = \left( \frac{\partial \mathbf{V}}{\partial \mathbf{R}_A} \right)^{\dagger} \mathbf{w} + \frac{1}{2} (\mathbf{V}^{\dagger} \mathbf{T}_{\varepsilon}^{-1})^{\dagger} \left[ \frac{\partial \mathbf{R}_{\infty}}{\partial \mathbf{R}_A} \mathbf{V} + \frac{\partial \mathbf{T}_{\varepsilon}}{\partial \mathbf{R}_A} \mathbf{q} \right], \quad (48)$$

where  $\mathbf{w}$  are the so-called polarization weights. This allows us to reuse the already existing code for the PCM gradient to compute the first term of the right hand side of Eq. (47) by replacing  $\mathbf{w}$  with  $\mathbf{q}$ ,  $(\mathbf{V}^{\dagger} \mathbf{T}_{\varepsilon}^{-1})$  with  $\tilde{\mathbf{q}}$ , and  $\mathbf{V}$  with  $(2\mathbf{V} + \mathbf{T}_{\varepsilon}^{\dagger} \tilde{\mathbf{q}})$ .

Note that, since the atomic positions  $\{\mathbf{R}_A\}$  and the  $\{\tilde{q}_{ij}\}$  are now two sets of independent variables, the first term on the right hand side of Eq. (47) does not assume that the polarization charges satisfy the PCM equations and thus it is not the complete derivative of the energy with respect to  $\{\mathbf{R}_A\}$ . Indeed, the latter assumes the form of Eq. (47) where two additional contributions are present.

### III. NUMERICAL EXAMPLES

The variational formalism introduced in section II has been implemented in a development version of the GAUSSIAN suite of programs.<sup>42</sup> In particular, we implemented the free energy functional in Eq. (43) and its derivatives in connection to MM methods. A MM geometry optimizer which alternates conjugate gradient and linear search steps has been generalized to handle simultaneously both geometrical and polarization variables, or only the geometrical variables when the PCM equations are solved for a given set of atomic coordinates. The universal force field (UFF) (Ref. 43) has been used throughout, both for gas phase and in solution calculations. The atomic charges have been determined using the QEq algorithm.<sup>44</sup> A scaled van der Waals surface is built around the solute using the UFF radii<sup>43</sup> scaled by a factor of 1.1. This choice of radii and scale factor usually leads to a cavity similar to the SES, at least in terms of total surface and volume. The discretization of the cavity surface is such that there are approximately five surface elements per Å<sup>2</sup>.

In the following, by *standard* calculation we indicate a calculation where the PCM equations as in Eq. (35) are solved, the gradient with respect to the atomic position of the corresponding free energy contribution is computed and used to decide the change in the solute's geometry. On the other hand, by *variational* calculation we indicate the case where the molecular geometry of the solvated system is obtained by simultaneous minimization of the energy functional in Eq. (43), which is used to compute the PCM energy contribution, while its first derivatives with respect to the atomic position are computed according to Eq. (47) and, at the same time, the first derivatives with respect to the polarization variables are evaluated as in Eq. (46). Both sets of derivatives are used to figure out the step in the space of both the atomic positions and the polarization degrees of freedom.

Tables I–IV collect the results for the standard and the variational formulations of PCM applied to the geometry optimization of a group of molecules in different solvents. The optimizations are performed with the conjugate gradient algorithm described above. Such algorithm, however, does not yet include any improvement that would make it more effective in performing simultaneous optimizations of atomic coordinates and polarization variables. The two groups of vari-

TABLE I. Comparison between standard and variational PCM calculations in water ( $\epsilon=78.36$ ): energies (millihartree), number of steps for the optimization ( $N_{\text{opt}}$ ), total number of matrix-vector products ( $N_{\text{mult}}$ ), and elapsed time (s). The calculations were performed on one six-core CPU AMD Opteron 8435. Et=Ethyl, Ph=Phenyl, PNA=*p*-nitroaniline.

Solute	Variational				Standard			
	Energy	$N_{\text{opt}}$	$N_{\text{mult}}$	Time	Energy	$N_{\text{opt}}$	$N_{\text{mult}}$	Time
H <sub>2</sub> CO	-8.3293	101	1140	36	-8.3293	7	1236	34
CH <sub>3</sub> COH	-31.8152	218	2398	162	-31.8152	41	10 992	339
CH <sub>3</sub> COCH <sub>3</sub>	-98.0786	282	3050	117	-98.0785	17	4224	125
EtCOCH <sub>3</sub>	-21.9940	313	3408	171	-21.9939	28	7758	291
EtCOEt	53.4225	316	3450	220	53.4225	35	10 656	493
PNA	-5.7194	198	2240	169	-5.7194	16	4494	245
PhCOH	21.2880	528	5576	338	21.2879	39	11 964	495
PhCOOH	2.1916	699	6828	443	2.1916	43	12 738	566
PhCOCH <sub>3</sub>	-0.8026	875	9034	687	-0.8025	47	13 938	810

ables are treated equally and no attempt has been made to differentiate them in order to obtain a more accurate step in either one variable subspace. Work in this direction is under way and will be reported in a separate communication.

The quantities we consider are the final energy in millihartree, the number of steps to reach the minimum ( $N_{\text{opt}}$ ), the total number of matrix-vector products ( $N_{\text{mult}}$ ), and the elapsed time. By matrix-vector product we indicate the operation of generating the required integrals and integral derivatives [as in Eq. (22)] and their contraction with a suitable vector. Before moving to the analysis of the results it is useful to comment on how  $N_{\text{mult}}$  is evaluated. In a standard calculation, the value of the polarization charges at each geometry optimization step is computed by solving the PCM equations iteratively, without storing any matrix of integrals in memory, but rather recalculating them as needed. This provides a fairer comparison with the variational approach, and it puts the prototypical calculations we are showing in the same conditions as those on a large system, where storing the integrals in memory would be too demanding. The number of matrix-vector products for each optimization step is computed considering that each iteration for the solution of the PCM problem requires six products, and six more products are required to evaluate the gradient of the free energy in solution with respect to the atomic coordinates, once the iterative solution has converged. On the other hand, for each optimization step in the variational approach, one product is required to evaluate the energy, three more to assemble the gradient with respect to the polarization variables, and again

six products are required to compute the gradients with respect to the atomic coordinates. In addition, the variational calculation includes a full solution of the PCM equations at the starting geometry to provide the initial values for the polarization variables.

The convergence criterion for the iterative solution of the PCM equations in the standard approach is such that both the root mean square (rms) and the maximum variation of the polarization charges are below  $10^{-9}$ . The convergence criteria for the atomic coordinates in the geometry optimization require that the maximum force is  $<1.125 \times 10^{-4}$ , the force rms is  $<7.5 \times 10^{-5}$ , the maximum displacement of a coordinate is  $<4.5 \times 10^{-4}$ , and the rms displacement is  $<3 \times 10^{-4}$ . In the case of the variational PCM calculation, the criteria for the convergence of the polarization variables are one order of magnitude smaller than the ones for the atomic coordinates. Note that these convergence criteria are strongly conservative as we aim to compare fully converged results from the standard and the variational calculations.

We point out that in the standard approach we need to achieve tight convergence on the charges before computing the gradient with respect to the geometrical degrees of freedom. One could consider using a looser convergence far from the minimum, but in such condition the energy would not be accurate enough to be used by the optimization algorithm, leading to a less effective and possibly problematic minimization. On the other hand, in the variational approach,

TABLE II. Comparison between standard and variational PCM calculations in dichloromethane ( $\epsilon=8.93$ ): energies (millihartree), number of steps for the optimization ( $N_{\text{opt}}$ ), total number of matrix-vector products ( $N_{\text{mult}}$ ), and elapsed time (s). The calculations were performed on one six-core CPU AMD Opteron 8435. Ph=Phenyl, PNA=*p*-nitroaniline.

Solute	Variational				Standard			
	Energy	$N_{\text{opt}}$	$N_{\text{mult}}$	Time	Energy	$N_{\text{opt}}$	$N_{\text{mult}}$	Time
PNA	-3.9839	147	1712	130	-3.9802	16	4332	235
PhCOH	22.4299	554	5824	351	22.4299	39	11 466	474
PhCOOH	3.3182	615	6416	415	3.3182	43	12 138	539
PhCOCH <sub>3</sub>	0.2493	882	9098	699	0.2495	47	12 696	691

TABLE III. Comparison between standard and variational PCM calculations in cyclohexane ( $\epsilon=2.02$ ): energies (millihartree), number of steps for the optimization ( $N_{\text{opt}}$ ), total number of matrix-vector products ( $N_{\text{mult}}$ ), and elapsed time (s). The calculations were performed on one six-core CPU AMD Opteron 8435. Ph=Phenyl, PNA=*p*-nitroaniline.

Solute	Variational				Standard			
	Energy	$N_{\text{opt}}$	$N_{\text{mult}}$	Time	Energy	$N_{\text{opt}}$	$N_{\text{mult}}$	Time
PNA	1.7545	267	2906	240	1.7546	11	2706	187
PhCOH	26.0835	673	7014	461	26.0835	39	10 980	540
PhCOOH	6.9794	663	6896	484	6.9795	41	11 322	601
PhCOCH <sub>3</sub>	3.5838	1039	10 644	868	3.5840	47	13 452	806

the free energy functional in Eq. (43) does not require at all convergence of the charges in order to compute with equal accuracy both the energy and the gradient.

We compared the free energy corresponding to the optimized geometry in solution according to both the PCM and C-PCM models in both standard and variational calculations. For this comparison, we used a very large dielectric constant ( $\epsilon=10^{12}$ ) to numerically confirm that the two methods are equivalent in the limit of  $\epsilon \rightarrow \infty$ . Indeed, they converged to the same minimum and the energy differences were consistently smaller than  $10^{-7}$  hartree. This represents an internal check of the correctness of the implementation.

Table I collects the results obtained for a group of small molecules, using both the standard and the variational formulation of PCM, and using water as solvent. As can be expected,  $N_{\text{opt}}$  is much smaller in the standard calculations, since the number of variables to be optimized (i.e., the atomic coordinates) is much smaller than in the variational calculations. Moreover, in the variational calculations the optimization algorithm shows very slow convergence on the polarization variables in the proximity of the minimum. This adds a significant number of steps to the variational optimization, where the geometry appears to be practically unchanged and the energy only changes by a very small amount. Notwithstanding the slow convergence, the overall number of matrix-vector products  $N_{\text{mult}}$  is definitely smaller in the variational calculations, especially for the larger molecules in the group. Accordingly, the elapsed time is favorable to the simultaneous optimization of geometry and polarization. Similar trends are observed when dichloromethane (i.e., a less polar solvent) is used. According to Table II, the variational PCM is faster than the traditional one for the first three solutes, while the timing is similar for PhCOCH<sub>3</sub> because of the large number of steps required by the variational approach. Again, very similar conclusions can be reached looking at Table III where the results using cyclohexane as

solvent are collected. In this case, also for *p*-nitro-aniline (PNA) the variational calculation is somewhat slower than the standard one.

In Table IV we report the results for a quite larger solute, i.e., tuftsin (Thr-Lys-Pro-Arg), using water as solvent. For this case we measured the differences between the optimized structure obtained with the standard and the variational approaches and we found a rms difference of  $<0.0001$  Å and a maximum difference of  $0.0005$  Å among the bond lengths, rms of  $<0.01^\circ$  and maximum difference of  $0.27^\circ$  among the bond angles, and rms of  $0.18^\circ$  and maximum of  $3.76^\circ$  among the dihedral angles. We emphasize that the elapsed time in Table IV is in hours. This example clearly shows the advantage of the variational approach over the standard one, especially considering that the number of optimization steps required by the variational calculations should be significantly reduced by an optimization algorithm that was aware of the two different sets of variables and capable of choosing better steps in each variable space. Moreover, as previously noted, in these examples we used strongly conservative convergence criteria. The use of less strict criteria is currently under investigation and initial results seem to be in favor of the use of the variational approach.

#### IV. CONCLUSIONS AND OUTLOOK

In this paper we introduce a new variational formulation of the PCM of solvation. Within such formulation the PCM charges, which represent the polarization of the dielectric continuum, become independent variables and are treated on the same footing as the position of the atoms of the solute and the solute's electronic density distribution. All these variables are used to define a free energy functional whose variational minimization leads to the free energy of the solute at its equilibrium geometry in solution. In particular, we demonstrated that such energy functional is free of discontinuities even when surface elements repeatedly emerge and start

TABLE IV. Comparison between standard and variational PCM calculations in water ( $\epsilon=78.36$ ): energies (millihartree), number of steps for the optimization ( $N_{\text{opt}}$ ), total number of matrix-vector products ( $N_{\text{mult}}$ ), and elapsed time (h). The calculations were performed on one six-core CPU AMD Opteron 8435.

Solute	Variational				Standard			
	Energy	$N_{\text{opt}}$	$N_{\text{mult}}$	Time	Energy	$N_{\text{opt}}$	$N_{\text{mult}}$	Time
Tuftsin	120.6882	5054	50 992	13.5	120.6517	384	201 204	30

to interact with the solute and the dielectric continuum, or become buried within the solute cavity. This property allows the functional to be effectively applied to the simultaneous minimization with respect to both geometry and polarization variables, and we conclude that the variational approach can compete successfully with the standard approach which alternates a solution of the PCM problem and a step in the solute geometry. We are working on improving existing optimization procedures to deal effectively with the different sets of variables involved in such simultaneous optimization problem, and on extending this approach to QM methods. Additionally, we are currently pursuing, with some promising early results, two other applications of the PCM free energy functional, namely, the simultaneous optimization of electronic density and polarization in the case of semiempirical method and the formulation and implementation of an extended Lagrangian MD approach, where the polarization degrees of freedom are characterized by a suitable fictitious mass and are propagated together with the solute atomic coordinates.

## ACKNOWLEDGMENTS

We thank Professor Berny H. Schlegel and Dr. Hrant Hratchian for helpful discussions. F.L. and B.M. gratefully acknowledge the financial support from Gaussian, Inc.

- <sup>1</sup>J. Tomasi, B. Mennucci, and R. Cammi, *Chem. Rev. (Washington, D.C.)* **105**, 2999 (2005).
- <sup>2</sup>*Continuum Solvation Models in Chemical Physics*, edited by B. Mennucci and R. Cammi (Wiley, New York, 2007).
- <sup>3</sup>C. Amovilli, V. Barone, R. Cammi, E. Cancès, M. Cossi, B. Mennucci, C. Pomelli, and J. Tomasi, *Quantum Systems in Chemistry and Physics*, Advances in Quantum Chemistry Vol. 32 (Academic Press, Inc., San Diego, 1999), Pt. II, p. 227.
- <sup>4</sup>J. Tomasi and M. Persico, *Chem. Rev. (Washington, D.C.)* **94**, 2027 (1994).
- <sup>5</sup>G. Scalmani and M. J. Frisch, *J. Chem. Phys.* **132**, 114110 (2010).
- <sup>6</sup>M. Caricato, G. Scalmani, and M. Frisch, in *Continuum Solvation Models in Chemical Physics*, edited by B. Mennucci and R. Cammi (Wiley, New York, 2007), Chap. 1.4, pp. 64–81.
- <sup>7</sup>D. York and M. Karplus, *J. Phys. Chem. A* **103**, 11060 (1999).
- <sup>8</sup>R. Allen, J. Hansen, and S. Melchionna, *Phys. Chem. Chem. Phys.* **3**, 4177 (2001).
- <sup>9</sup>L. D. Landau and E. M. Lifshitz, *Electrodynamics of Continuous Media* (Pergamon, Oxford, 1960).
- <sup>10</sup>B. U. Felderhof, *J. Chem. Phys.* **67**, 493 (1977).
- <sup>11</sup>M. Marchi, D. Borgis, N. Levy, and P. Ballone, *J. Chem. Phys.* **114**, 4377 (2001).
- <sup>12</sup>T. HaDuong, S. Phan, M. Marchi, and D. Borgis, *J. Chem. Phys.* **117**, 541 (2002).
- <sup>13</sup>P. Attard, *J. Chem. Phys.* **119**, 1365 (2003).
- <sup>14</sup>P. Attard, *J. Chem. Phys.* **127**, 129901 (2007).
- <sup>15</sup>A. Klamt and G. Schuurmann, *J. Chem. Soc., Perkin Trans. 2* **1993**, 799.
- <sup>16</sup>V. Barone and M. Cossi, *J. Phys. Chem. A* **102**, 1995 (1998).
- <sup>17</sup>S. Dapprich, I. Komáromi, K. Suzie Byun, K. Morokuma, and M. J. Frisch, *J. Mol. Struct.: THEOCHEM* **461–462**, 1 (1999).
- <sup>18</sup>T. Vreven, K. S. Byun, I. Komaromi, S. Dapprich, J. Montgomery, A. John, K. Morokuma, and M. J. Frisch, *J. Chem. Theory Comput.* **2**, 815 (2006).
- <sup>19</sup>T. Vreven, B. Mennucci, C. da Silva, K. Morokuma, and J. Tomasi, *J. Chem. Phys.* **115**, 62 (2001).
- <sup>20</sup>T. Vreven, K. Morokuma, O. Farkas, H. Schlegel, and M. Frisch, *J. Comput. Chem.* **24**, 760 (2003).
- <sup>21</sup>G. Scalmani, M. Frisch, B. Mennucci, J. Tomasi, R. Cammi, and V. Barone, *J. Chem. Phys.* **124**, 094107 (2006).
- <sup>22</sup>R. Cammi, *J. Chem. Phys.* **131**, 164104 (2009).
- <sup>23</sup>M. Caricato, B. Mennucci, G. Scalmani, G. W. Trucks, and M. J. Frisch, *J. Chem. Phys.* **132**, 084102 (2010).
- <sup>24</sup>F. Lipparini, G. Scalmani, and B. Mennucci, *Phys. Chem. Chem. Phys.* **11**, 11617 (2009).
- <sup>25</sup>H. Senn, P. Margl, R. Schmid, T. Ziegler, and P. Blochl, *J. Chem. Phys.* **118**, 1089 (2003).
- <sup>26</sup>R. Car and M. Parrinello, *Phys. Rev. Lett.* **55**, 2471 (1985).
- <sup>27</sup>H. Schlegel, J. Millam, S. Iyengar, G. Voth, A. Daniels, G. Scuseria, and M. Frisch, *J. Chem. Phys.* **114**, 9758 (2001).
- <sup>28</sup>J. D. Jackson, *Classical Electrodynamics*, 3rd ed. (Wiley, New York, 1999).
- <sup>29</sup>E. Cancès and B. Mennucci, *J. Math. Chem.* **23**, 309 (1998).
- <sup>30</sup>B. Mennucci, E. Cancès, and J. Tomasi, *J. Phys. Chem. B* **101**, 10506 (1997).
- <sup>31</sup>W. Hackbusch, *Integral Equations—Theory and Numerical Treatment* (Birkhäuser, Basel, 1995).
- <sup>32</sup>D. Chipman, *J. Chem. Phys.* **110**, 8012 (1999).
- <sup>33</sup>E. Cancès, in *Continuum Solvation Models in Chemical Physics*, edited by B. Mennucci and R. Cammi (Wiley, New York, 2007), Chap. 1.2, pp. 29–48.
- <sup>34</sup>M. Cossi, G. Scalmani, N. Rega, and V. Barone, *J. Chem. Phys.* **117**, 43 (2002).
- <sup>35</sup>A. W. Lange and J. M. Herbert, *J. Phys. Chem. Lett.* **1**, 556 (2010).
- <sup>36</sup>E. Cancès, B. Mennucci, and J. Tomasi, *J. Chem. Phys.* **107**, 3032 (1997).
- <sup>37</sup>D. Chipman, *J. Chem. Phys.* **124**, 224111 (2006).
- <sup>38</sup>M. Cossi, N. Rega, G. Scalmani, and V. Barone, *J. Chem. Phys.* **114**, 5691 (2001).
- <sup>39</sup>M. Cossi, N. Rega, G. Scalmani, and V. Barone, *J. Comput. Chem.* **24**, 669 (2003).
- <sup>40</sup>G. Scalmani, V. Barone, K. Kudin, C. Pomelli, G. Scuseria, and M. Frisch, *Theor. Chem. Acc.* **111**, 90 (2004).
- <sup>41</sup>J. L. Pascual-ahuir, E. Silla, and I. Tuñón, *J. Comput. Chem.* **15**, 1127 (2004).
- <sup>42</sup>M. J. Frisch, G. W. Trucks, H. B. Schlegel *et al.*, GAUSSIAN, Revision H.07, Gaussian, Inc., Wallingford, CT, 2010.
- <sup>43</sup>A. Rappe, C. Casewit, K. Colwell, W. Goddard, and W. Skiff, *J. Am. Chem. Soc.* **114**, 10024 (1992).
- <sup>44</sup>A. Rappe and W. Goddard, *J. Phys. Chem.* **95**, 3358 (1991).